



Prediction of upgrade to clinically significant prostate cancer in patients under active surveillance: Performance of a fully automated AI-algorithm for lesion detection and classification

Benedict Oerther MD¹  | Hannes Engel MD¹  | Andrea Nedelcu MD¹ | Christopher L. Schlett MD¹ | Robert Grimm PhD² | Heinrich von Busch PhD³ | August Sigle MD⁴ | Christian Gratzke MD⁴ | Fabian Bamberg MD¹ | Matthias Benndorf MD, PD¹

¹Department of Radiology, Medical Center-University of Freiburg, Faculty of Medicine, University of Freiburg, Freiburg, Germany

²MR Application Development, Siemens Healthcare GmbH, Erlangen, Germany

³Diagnostic Imaging Digital & Automation, Siemens Healthcare GmbH, Erlangen, Germany

⁴Department of Urology, Medical Center-University of Freiburg, Faculty of Medicine, University of Freiburg, Freiburg, Germany

Correspondence

Benedict Oerther, Department of Radiology, Medical Center-University of Freiburg, Faculty of Medicine, University of Freiburg, Hugstetter Straße 55, 79106 Freiburg, Germany.

Email: benedict.oerther@uniklinik-freiburg.de

Abstract

Background: Multiparametric MRI (mpMRI) improves the detection of aggressive prostate cancer (PCa) subtypes. As cases of active surveillance (AS) increase and tumor progression triggers definitive treatment, we evaluated whether an AI-driven algorithm can detect clinically significant PCa (csPCa) in patients under AS.

Methods: Consecutive patients under AS who received mpMRI (PI-RADSv2.1 protocol) and subsequent MR-guided ultrasound fusion (targeted and extensive systematic) biopsy between 2017 and 2020 were retrospectively analyzed. Diagnostic performance of an automated clinically certified AI-driven algorithm was evaluated on both lesion and patient level regarding the detection of csPCa.

Results: Analysis of 56 patients resulted in 93 target lesions. Patient level sensitivity and specificity of the AI algorithm was 92.5%/31% for the detection of ISUP \geq 1 and 96.4%/25% for the detection of ISUP \geq 2, respectively. The only case of csPCa missed by the AI harbored only 1/47 Gleason 7a core (systematic biopsy; previous and subsequent biopsies rendered non-csPCa).

Conclusions: AI-augmented lesion detection and PI-RADS scoring is a robust tool to detect progression to csPCa in patients under AS. Integration in the clinical workflow can serve as reassurance for the reader and streamline reporting, hence improve efficiency and diagnostic confidence.

KEYWORDS

active surveillance, artificial intelligence, clinically significant prostate cancer, lesion detection and classification, PI-RADSv2.1, prostate cancer

1 | INTRODUCTION

Multiparametric MRI of the prostate (mpMRI) has become a fundamental tool in the diagnostic pathway of prostate cancer (PCa) and was consequently implemented in several internationally recognized guidelines.^{1–4} With rising demand for exams, the required workforce for the reading of prostate MRI also increases—thus presenting an organizational challenge for efficient clinical reporting. Artificial intelligence (AI) based lesion detection and classification in prostate MRI has emerged as a promising technique to make reading of prostate MRI exams more time efficient⁵ with improved interobserver agreement and at least the same diagnostic accuracy compared to radiologists.^{6,7}

Due to the heterogeneity in histopathological subtypes of PCa, prognosis and therapy differ enormously depending on histopathological subtype as well-differentiated (low-grade) tumors show less aggressive growth and better prognosis.⁸ The majority of PCa are rather slow-growing and potentially clinically inapparent.⁹ For instance, clinically insignificant tumors (ncsPCa) in low-risk settings do not require immediate treatment but can be monitored in active surveillance (AS).¹⁰ However, a proportion can present with an aggressive growth rate, limiting the patient's life span and calling for different lines of therapy which results in the need to distinguish one type from the other.¹¹ MpMRI improves detection of aggressive PCa that calls for prompt treatment^{12–15} and is a strong predictor for tumor progression under AS.^{16,17}

The current reading practice of prostate MRI and the expected increasing number of AS cases undergoing MRI¹⁸ makes an intensification of the radiological workload in the near future foreseeable. AI driven reporting might serve as a tool to dampen the rise in cost and human resources. If clinically significant PCa (csPCa) can be detected reliably and fit in a structured report by automated algorithms, the reporting process can be streamlined and provide reinforcing feedback for the interpreting radiologist.

The purpose of this study was to evaluate whether a clinically certified AI-driven lesion detection algorithm can detect csPCa in patients under AS and therefore increase efficiency and confidence in clinical decision making.

2 | METHODS

2.1 | Subjects

In this single-center retrospective study we evaluated 56 consecutive patients who received mpMRI of the prostate between April 2017 and February 2020 while being under AS. Median age was 63 years (range: 54–78; mean: 67.23; SD: 5.74). Indications for MRI during AS were suspicion for progression due to prostate specific antigen (PSA)-dynamic ($n = 31$; mean PSA doubling time: 50.6 months; mean PSA slope: 0.18, mean PSA velocity: 4.7 ng/mL/month), standard procedure during AS with nonincreasing PSA and MR-guided surveillance biopsy ($n = 18$), patient request ($n = 1$), and unknown reasons ($n = 6$). PSA-dynamics were calculated considering the two most recent

mpPSA values before the MRI using an open-access online tool.¹⁹ Follow-up MRI and rebiopsy as standard procedure in AS were performed in patients who received initial MRI scans and systematic (\pm targeted) biopsy before inclusion or in case there was no initial MRI available according to international guidelines.^{1,3} Patients were excluded if MRI exams were performed for first guided biopsy before AS, even if the biopsies resulted in AS. Median PSA before biopsy was 9.48 ng/mL (range: 0.55–63.89; mean: 11.18; SD: 9.58). All patients underwent TRUS-fusion guided biopsy (targeted and systematic) for histopathological verification subsequently.

2.2 | MRI reading and protocol

MpMRI of the prostate was read by board-certified radiologists according to the PI-RADS (Prostate Imaging Reporting and Data System) lexicon, which establishes a standardized diagnostic approach²⁰ and works well as a risk stratification tool in the detection of PCa.^{21,22} As PI-RADS formally does not address MRI for evaluation of progression during AS,²⁰ examinations were evaluated based on PI-RADS criteria but did not receive a final score. Instead, all potentially cancerous lesions were marked and described for confirmation biopsy.

All exams were acquired in the same 3T scanner (MAGNETOM Vida; Siemens Healthcare) according to the PI-RADSV2.1 acquisition protocol: T2 weighted images with 3 mm slice thickness and no gap (2D TSE, TR: 7500 ms, TE: 104 ms, FA: 160°). The field-of-view was 200 × 200 mm (768 × 768 matrix), in-plane resolution was 0.26 × 0.26 mm.²⁰ No endorectal coil was used. Butylscopolamine was injected intravenously before the scan with dose adjustment considering body weight. Acquired images were then prepared for MRI-ultrasound fusion biopsies. Both the prostate gland and scored lesions were segmented manually by a trained radiologist in axial T2 weighted slices under the supervision of a board-certified radiologist. For the current study, we recorded all lesions described as suspicious by the interpreting radiologist in clinical routine.

2.3 | Histopathological verification

MRI-guided ultrasound fusion transperineal biopsy was performed and accomplished with the MonaLisa environment (Biobot Surgical Pte Ltd). Laryngeal mask anesthesia was established periprocedurally. A three-dimensional model of the prostate gland was generated by the endorectal ultrasound probe and fused with the MR volume derived by manual segmentation of T2 weighted imaging by a specialized urologist. Lesions previously defined and scored by the radiologist were transferred to the in vivo ultrasound model. Transperineal access for biopsy was established by incision. Biopsy angle and depth were automatically calculated by the software. An automated imaging-guided robotic arm was then positioned for biopsy. A multiuse biopsy device (Uromed; REF6020) and trocar-like needles (Uromed; REF 6025.10) were used and triggered manually. Target lesion biopsies were performed before systematic biopsies.

Systematic biopsies were taken according to the volume adapted Ginsburg study scheme.²³ Patients received postprocedural transurethral catheterization. For a detailed description of the biopsy procedure refer to the publication of Kroenig et al.²⁴

2.4 | AI-algorithm

An AI-driven, CE-certified research software for detection of prostate lesions based on bi-parametric MRI (MR Prostate AI v1.3.2, build date 2021-11-15; Siemens Healthcare) was used for automatic detection, segmentation, and classification of prostate lesions.

The AI model, which is based on bi-parametric MRI, has been described extensively in a previous publication.⁶ Briefly summarized, it comprises preprocessing by an automatic segmentation of the prostate gland on axial T2-weighted imaging (T2WI) and diffusion-weighted imaging (DWI), followed by coregistration of T2WI and DWI. From the DWI series, a synthetic *b*-value image at *b* = 2000 s/mm² and an ADC map are computed. The segmentation, as well as the coregistered T2WI, *b* = 2000 image and ADC map, are then fed into a 2D image-to-image convolutional neural network (CNN), producing an initial map of suspicious lesions. These lesion candidates are then processed by a second CNN stage, performing a 3D patch-wise classification for false positive reduction.²⁵ Finally, a PI-RADS score proposal is automatically deduced from the network's response and the detected lesion's diameter.

2.5 | Definitions and criteria

csPCa was defined based on histopathology defined ISUP grade or Gleason score as ISUP ≥ 2 .²⁶ International guidelines state inclusion criteria for AS as follows: life expectancy ≥ 10 years, PSA-values ≤ 10 ng/mL, Gleason-score ≤ 6 , cT1 and cT2a tumor stages, tumor cells in ≤ 2 cores and in case of $\leq 50\%$ tumor per core.^{1,3,27–29} However, we exclusively included patients with biopsy proven low risk PCa (ISUP 1).

2.6 | Data collection

The patient cohort was derived from our local database and filtered for previously known malignancy of the prostate. Thereafter clinical records were searched, and if needed, additional clinical information from the Department of Urology was requested. Ethical approval was obtained beforehand by the local ethics committee.

3 | RESULTS

3.1 | Biopsy

Analysis of 56 patients resulted in a total of 93 detected lesions. Eighty-three lesions were accessible for targeted biopsy. Ten lesions

did not receive targeted biopsy due to difficulties in coregistration of ultrasound to MR imaging, low lesion volume and location directly adjacent to larger target lesions. On average, 2.7 cores were acquired per target (range 1–12; median: 3). Mean number of cores in the additionally performed systematic biopsy was 28.8 (range: 15–58; median: 29), the (volume adapted) Ginsburg biopsy scheme was used for systematic biopsies.²³

3.2 | Lesion level analysis

Of 83 lesions detected by the radiologists, 49/83 (59%) targets yielded ISUP 0, 7/83 (8%) ISUP 1, and 27/83 (33%) ISUP \geq ISUP 2. AI rated 54 lesions in accordance with the radiology reports (\geq PI-RADS 3; not every detected lesion had a corresponding targeted biopsy). AI assigned a PI-RADS score of 3 in 7 lesions of which 4 turned out to harbor no PCa (ISUP 0), 2 showed insignificant PCa (ISUP 1) and 1 significant PCa (ISUP ≥ 2). A PI-RADS score of 4 was assigned 18 times with 9 ISUP 0 lesions, 3 ISUP 1 lesions, and 4 ISUP ≥ 2 lesions (2 lesions were missing corresponding targeted biopsy). Twenty-nine PI-RADS 5 scores resulted in 8 ISUP 0 lesions, 1 ISUP 1 lesion, and 16 ISUP ≥ 2 lesions (4 lesions were missing corresponding targeted biopsy). Of the remaining 39 targeted lesions that were assigned PI-RADS 0 categories (i.e., not detected by the AI), 28 lesions were correctly identified as benign, while 1 ISUP 1 lesion and 6 ISUP ≥ 2 lesions were falsely classified as negative by AI (4 lesions were missing corresponding targeted biopsy). For detailed information refer to Figure 1.

3.3 | Patient level analysis

Based on mpMRI, AI classified 1/56 patients as PI-RADS 3, 7/56 were classified as PI-RADS 4, and 40/56 as PI-RADS 5. Eight patients were classified as benign.

Five out of 8 patients that were classified as negative by the AI proved benign after biopsy (systematic and targeted biopsy), 2 patients yielded ISUP 1 and 1 lesion ISUP ≥ 2 , respectively. One maximum AI-based PI-RADS score of 3 was assigned and proved to be ISUP 0. Of 7 patients with a maximum AI-based PI-RADS score of 4, 1 proved to be ISUP 0 and ISUP 1 each, while 5 patients showed ISUP ≥ 2 . The largest group of 39 patients scored as PI-RADS 5 by AI presented with 9, 9 and 22 ISUP 0, ISUP 1, and ISUP ≥ 2 grades, respectively. AI detected a mean of 1.11 additional lesions (lesions not overlapping with manually detected lesions) per patient (0–5 lesions; median: 1; SD: 1.23). Corresponding data is presented in Figure 2.

Overall, the patient level sensitivity/specificity of the AI algorithm was 92.5% (37/40)/31% (5/16) for detection of ISUP 1 or higher, and 96.4% (27/28)/25% (7/28) for detection of ISUP 2 or higher.

Two cases of nsPCa were neither detected by the radiologist nor the AI. In one, patient 1 of 2 cores of targeted biopsy as well as 3 of

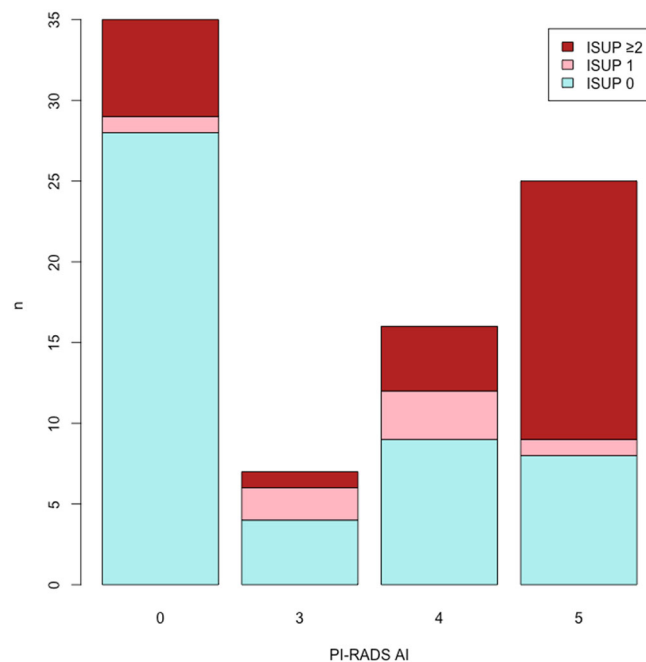


FIGURE 1 Lesion level analysis (lesions \geq PI-RADS 3 with corresponding targeted biopsy cores only); PI-RADS 0 means the lesion was not detected by AI. PI-RADS, prostate imaging reporting and data system. [Color figure can be viewed at wileyonlinelibrary.com]

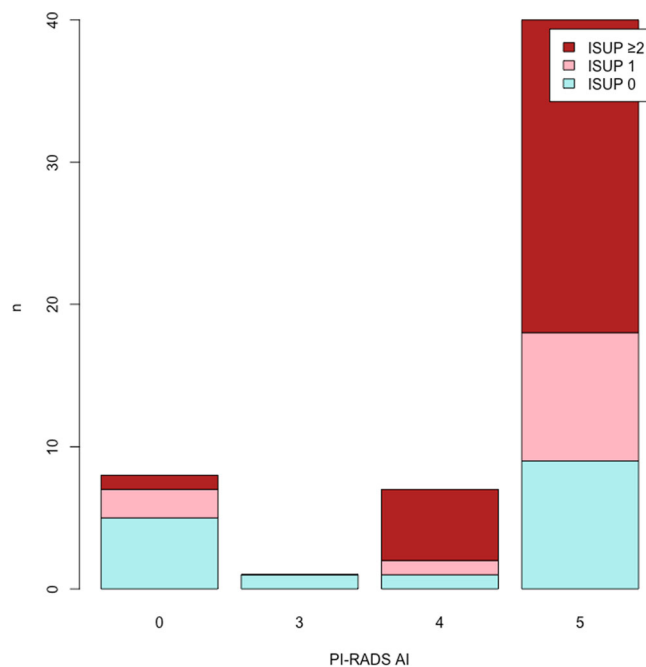


FIGURE 2 Patient level analysis. An AI-based PI-RADS score of 0 means the patient was classified as negative. PI-RADS, prostate imaging reporting and data system. [Color figure can be viewed at wileyonlinelibrary.com]

22 random biopsy cores yielded a Gleason 3 + 3 pattern (ISUP 1), the other one did not receive targeted biopsy but presented with 1 of 33 cores with Gleason 3 + 3 pattern in random biopsy.

One patient harbored Gleason 3 + 4 in one systematic core and Gleason 3 + 3 in two cores out of 47 (negative target lesions) and was not detected by AI (for details compare Figure 2).

Detailed histopathology results are depicted in Table 1. Compare for Figures 3–5 for examples of a true positive, a true negative, and the previously mentioned false negative result.

4 | DISCUSSION

Overall, AI achieved an excellent sensitivity for the detection of csPCa on patient level (92.5% ISUP \geq 1; 96.4% ISUP \geq 2) with only one debatable case of csPCa missed (refer to Figure 2) but low specificity (31.5% ISUP \geq 1; 25% ISUP \geq 2). These results fit the intention to detect csPCa in particular, so that in a clinical setting almost no critical case would be missed. This partially reflects findings of other authors who showed equally high sensitivity levels but also better specificity: Fehr et al. reported accuracies up to 93% for the distinction between ISUP 1 and ISUP $>$ 1 cancers with integration of imaging features³⁰ although applied to a non-AS cohort with inclusion of patients with known PCa; Antonelli et al. developed a model that showed sensitivities up to 88% (at 50% specificity threshold) and even outperformed board-certified radiologists in differentiating tumors with and without a Gleason 4 component.³¹ Deviations in specificity most likely derive from our patient cohort, being a high-risk population under AS, entirely receiving prostate MRI and subsequent MRI guided biopsy.

Detected lesions in our cohort showed predominantly Gleason Grade (GG) \geq 2 in histopathology although AS is proposed for patients with clinically insignificant carcinoma (GG \leq 1). Hamdy et al. reported 77% ISUP 1 cases and 23% ISUP \geq 2 cases in their cohort selected for AS with localized PCa.⁹ Arif et al. found a distribution on patient level of 53% ISUP 1 cases and 47% ISUP \geq 2 cases in their AS cohort³² compared to 12/56 (21%) and 28/56 (50%) in our cohort, although their study is only partially comparable since indication for mpMRI was not explicitly stated. This could originate from the indication for prostate MRI in our cohort, which was mainly suspected progression due to PSA-elevation. The proportion of intermediate risk tumors in other cohorts was found to be 18.9% (definition: Gleason 7 or T3 or PSA $>$ 15 ng/mL³³) compared to our cohort that consisted of 29% (16/56). Therefore, we conclude that we predominantly included high-risk patients with a more than average risk of progression into csPCa who in reality represent a subset of the overall AS cohort.

There are some heterogeneous studies that investigate tumor progression rates in cohorts with a substantial proportion of csPCa. Despite slight differences in the definitions of tumor progression (mostly including Gleason 4 as predominant histological subtype),

TABLE 1 Distribution of PI-RADS score assigned by the AI and corresponding histopathology result.

	Pi-RADS category assigned by AI	Corresponding Gleason score (n)				Total
		Benign	3 + 3	3 + 4	≥4 + 3	
Lesion level	0	28	1	6	0	35
	3	4	2	1	0	7
	4	9	3	4	0	16
	5	8	1	7	8	25
			49	7	18	9
Patient level	0	5	2	1	0	8
	3	1	0	0	0	1
	4	1	1	4	1	7
	5	9	9	14	8	40
			16	12	19	9

Abbreviation: PI-RADS, prostate imaging reporting and data system.

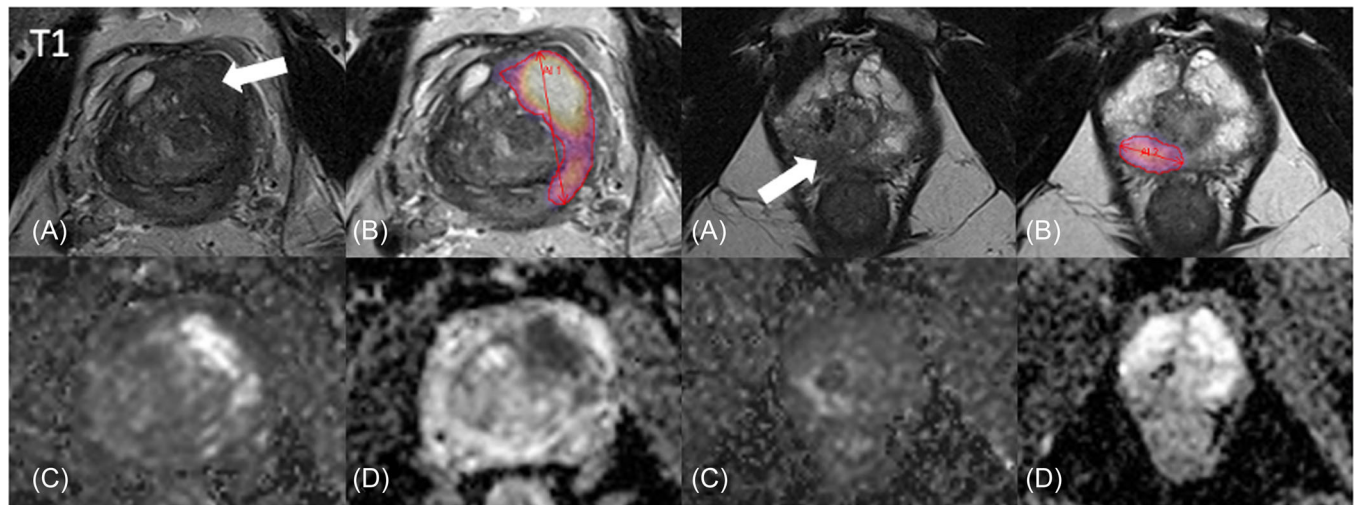


FIGURE 3 Example of a true positive result. AI detected both target lesions correctly and assigned PI-RADS 5 for both target lesions. Target lesion 1 (left) contained 4 Gleason 4 + 4 (predominantly 3 + 4, with a 4 + 4 component) out of 5 cores, target lesion 2 (right) contained 3 Gleason 4 + 4 out of 4 cores. Random biopsy yielded 2 Gleason 3 + 3, 4 Gleason 3 + 4, and 8 Gleason >3 + 4 cores out of 26. PSA at biopsy was 30.8 ng/mL. (A) Axial T2 weighted image; (B) axial T2 weighted image + heatmap overlay (AI output); (C) calculated high *b*-values; (D) ADC map; arrows: target lesions according to the radiology report. PI-RADS, prostate imaging reporting and data system; PSA, prostate specific antigen. [Color figure can be viewed at wileyonlinelibrary.com]

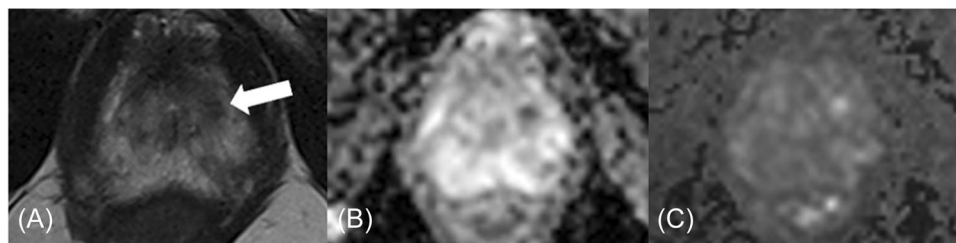


FIGURE 4 True negative result. AI correctly assigned a PI-RADS score of 0. Neither target nor random cores yielded PCa. PSA at biopsy was 5.7 ng/mL. (A) Axial T2 weighted image; (B) ADC map; (C) calculated high *b*-values; arrows: target lesions according to the radiology report. PCa, prostate cancer; PI-RADS, prostate imaging reporting and data system; PSA, prostate specific antigen.

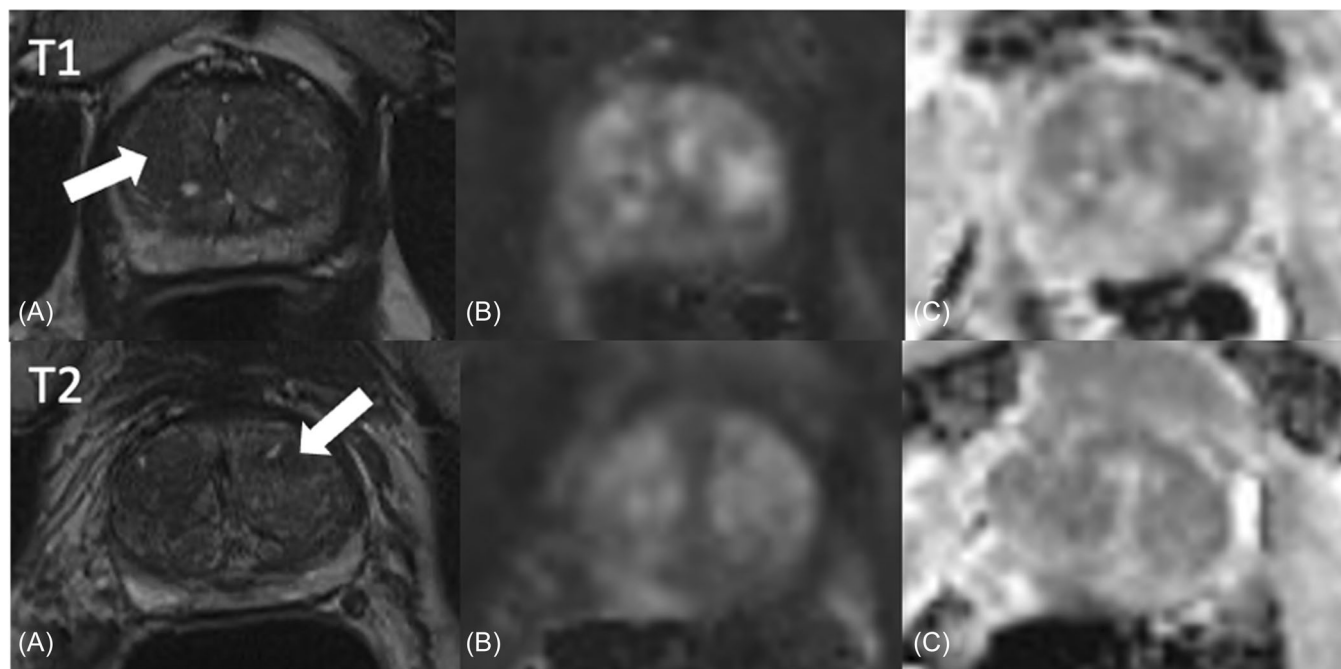


FIGURE 5 False negative result. AI assigned a PI-RADS score of 0. Two cores yielded Gleason 3 + 3 + 3 = 6 and 1 out of 47 random cores yielded Gleason-score 3 + 4 = 7a, hence significant PCa was missed. PSA at biopsy was 9.51. Initial biopsies yielded 1/11 Gleason 3 + 3, following biopsies before and after said images showed benign histopathology (35–47 cores each). (A) Axial T2 weighted image; (B) calculated high *b*-values; (C) ADC map; arrows: target lesions according to the radiology report. PCa, prostate cancer; PI-RADS, prostate imaging reporting and data system; PSA, prostate specific antigen.

previous studies found tumor progression rates of 19%–34%^{34–38} with no difference in outcome between Gleason 6 and Gleason 7 patients. The proportion of Gleason $\geq 4 + 3$ in our cohort was 16% (9/56). Moreover, PCa detected by established predictors of tumor progression such as PSA level elevation alone often results in higher false-positive rates, thus causing excess costs and potential risks related to unnecessary biopsies.³⁹ Recent studies do not only suggest that AI-based algorithms derived from mpMRI are able to differentiate between ncsPCa, csPCa, and benign prostatic alterations⁴⁰ and are capable of detecting tumors on histopathological level comparable to expert pathologists⁴¹ but could already show advances in false positive reduction²⁵ which gains importance rapidly with 25% PCa per PSA elevation (>4 ng/mL⁴²) and a total of estimated 1.4 million diagnoses worldwide in 2020.⁴³

The use of AS has increased drastically over the last decades, for example, from 14.5% in 2010 to 42.1% in 2015 in the US population.⁴⁴ Furthermore, recent international guidelines (AUA) already suggest AS for patients with low risk localized cancer and recommend discussion of AS for a favorable intermediate risk setting.⁴⁵ European guidelines (EAU) provide a weak recommendation for the inclusion of a favorable subset of ISUP 2 patients in AS.¹ Willems et al. also suggested less restrictive inclusion criteria in debatable cases of low-volume ISUP 2 patients. For instance, only high-volume ISUP 2 PCa or low-volume ISUP 2 PCa in combination with increased core positivity or core involvement should lead to active treatment.⁴⁶ This implies tendencies for rising numbers of AS cases in the future. Potential use cases for AI as reinforcement in

diagnostic confidence as second reader and triage tools were already suggested in the past.^{47,48} Thus, AI-aided detection and lesion scoring offers an additional noninvasive tool based on parameters that are already being acquired in the scanning process without additional expenditure of time.

As mentioned in Section 2, we did not assign PI-RADS scores to the target lesions detected by the reader as recommended by the PI-RADS lexicon (“[PI-RADSV2.1] does not address the use of MRI for detection of suspected recurrent prostate cancer following therapy [and] progression during surveillance”).²⁰ However, the employed AI automatically allocates PI-RADS scores to detected lesions depending on the estimated probability of present csPCa. Due to this intrinsic metric, we did not employ additional scoring systems (e.g., Likert scaling). We provide the distribution of AI assigned PI-RADS categories on lesion level and patient level. As intended for the standard use case of PI-RADS, cancer detection rates increase with higher PI-RADS categories (c.f. Figures 1 and 2). This provides initial evidence that the scope of the tested AI-driven lesion detection and classification may be successfully extended. However, since we tested the tool on a particularly specific patient collective it remains unclear whether the same performance can be achieved in a more heterogeneous setting with more benign exams, lower risk PI-RADS cases and especially in borderline cases of PI-RADS 3 or upgraded lesions.

AI performance was tested on and acquired from a rather small cohort in a retrospective single-institution environment, thus results need to be verified in a larger prospective cohort, ideally in a multicenter setting.

5 | CONCLUSION

We conclude that AI-augmented lesion detection and PI-RADS scoring is a robust tool to detect progression to cSPCa in patients under AS. Upon integration in the clinical workflow the tool can serve as reassurance for the reader and streamline reporting, hence improving diagnostic confidence, although additional multicenter studies need to evaluate the detection rates in both primary PCa diagnostics and AS cohorts. Once the AI tool achieves a sufficiently high negative predictive value, implementation as a rule-out test seems conceivable. In anticipation of further evidence for the implementation of AI, prostate MRI in AS could be analyzed by AI before human evaluation in future scenarios, therefore rendering the process more time efficient.

ACKNOWLEDGMENTS

Open Access funding enabled and organized by Projekt DEAL.

CONFLICT OF INTEREST STATEMENT

The authors declare no conflict of interest.

DATA AVAILABILITY STATEMENT

The data that support the findings of this study are available on request from the corresponding author. The data are not publicly available due to privacy or ethical restrictions.

ORCID

Benedict Oerther  <http://orcid.org/0000-0003-4267-3601>

Hannes Engel  <http://orcid.org/0000-0003-1985-325X>

REFERENCES

- EAU Guidelines. Edn. presented at the EAU Annual Congress Amsterdam ISBN 978-94-92671-16-5. 2022.
- Eastham JA, Auffenberg GB, Barocas DA, et al. Clinically localized prostate cancer: AUA/ASTRO guideline part II: principles of active surveillance, principles of surgery and follow-up. *J Urol*. 2022;208:19-25. doi:10.1097/JU.0000000000002758
- Leitlinienprogramm Onkologie (Deutsche Krebsgesellschaft, Deutsche Krebshilfe, AWMF): S3-Leitlinie Prostatakarzinom, Langversion 6.2, 2021, AWMF Registernummer: 043/022OL. 2021.
- Schoots IG, Padhani AR. Delivering clinical impacts of the MRI diagnostic pathway in prostate cancer diagnosis. *Abdominal Radiol*. 2020;45(12):4012-4022.
- Hötter AM, Da Mutten R, Tiessen A, Konukoglu E, Donati OF. Improving workflow in prostate MRI: AI-based decision-making on biparametric or multiparametric MRI. *Insights Imaging*. 2021;12(1):112.
- Winkel DJ, Tong A, Lou B, et al. A novel deep learning based computer-aided diagnosis system improves the accuracy and efficiency of radiologists in reading biparametric magnetic resonance images of the prostate: results of a multireader, multicase study. *Invest Radiol*. 2021;56(10):605-613.
- Van Booven DJ, Kuchakulla M, Pai R, et al. A systematic review of artificial intelligence in prostate cancer. *Res Rep Urol*. 2021;13:31-39.
- Lopez-Beltran A, Mikuz G, Luque RJ, Mazzucchelli R, Montironi R. Current practice of Gleason grading of prostate carcinoma. *Virchows Arch*. 2006;448(2):111-118.
- Hamdy FC, Donovan JL, Lane JA, et al. 10-year outcomes after monitoring, surgery, or radiotherapy for localized prostate cancer. *N Engl J Med*. 2016;375(15):1415-1424.
- Bill-Axelsson A, Holmberg L, Ruutu M, et al. Radical prostatectomy versus watchful waiting in early prostate cancer. *N Engl J Med*. 2011;364(18):1708-1717.
- Epstein JI. Pathologic and clinical findings to predict tumor extent of nonpalpable (stage T1c) prostate cancer. *JAMA: J Am Med Assoc*. 1994;271(5):368-374.
- Dieffenbacher S, Nyarangi-Dix J, Giganti F, et al. Standardized magnetic resonance imaging reporting using the prostate cancer radiological estimation of change in sequential evaluation criteria and magnetic resonance imaging/transrectal ultrasound fusion with transperineal saturation biopsy to select men on active surveillance. *European Urol Focus*. 2021;7(1):102-110.
- Gallagher KM, Christopher E, Cameron AJ, et al. Four-year outcomes from a multiparametric magnetic resonance imaging (MRI)-based active surveillance programme: PSA dynamics and serial MRI scans allow omission of protocol biopsies. *BJU Int*. 2019;123(3):429-438.
- Moore CM, Petrides N, Emberton M. Can MRI replace serial biopsies in men on active surveillance for prostate cancer? *Curr Opin Urol*. 2014;24(3):280-287.
- Sato C, Naganawa S, Nakamura T, et al. Differentiation of noncancerous tissue and cancer lesions by apparent diffusion coefficient values in transition and peripheral zones of the prostate. *J Magn Reson Imaging*. 2005;21(3):258-262.
- Mamawala MK, Meyer AR, Landis PK, et al. Utility of multiparametric magnetic resonance imaging in the risk stratification of men with Grade Group 1 prostate cancer on active surveillance. *BJU Int*. 2020;125(6):861-866.
- Schoots IG, Moore CM, Rouvière O. Role of MRI in low-risk prostate cancer: finding the wolf in sheep's clothing or the sheep in wolf's clothing? *Curr Opin Urol*. 2017;27(3):238-245.
- Kang SK, Mali RD, Prabhu V, Ferket BS, Loeb S. Active surveillance strategies for low-grade prostate cancer: comparative benefits and cost-effectiveness. *Radiology*. 2021;300(3):594-604.
- Nedeia D. PSA doubling time calculator. 2023.
- Turkbey B, Rosenkrantz AB, Haider MA, et al. Prostate imaging reporting and data system version 2.1: 2019 update of prostate imaging reporting and data system version 2. *Eur Urol*. 2019;76(3):340-351.
- Oerther B, Engel H, Bamberg F, Sigle A, Gratzke C, Benndorf M. Cancer detection rates of the PI-RADSv2.1 assessment categories: systematic review and meta-analysis on lesion level and patient level. *Prostate Cancer Prostatic Dis*. 2021;25(2):256-263.
- Park KJ, Choi SH, Kim M, Kim JK, Jeong IG. Performance of prostate imaging reporting and data system version 2.1 for diagnosis of prostate cancer: a systematic review and meta-analysis. *J Magn Reson Imaging*. 2021;54(1):103-112.
- Kuru TH, Wadhwa K, Chang RTM, et al. Definitions of terms, processes and a minimum dataset for transperineal prostate biopsies: a standardization approach of the Ginsburg Study Group for enhanced prostate diagnostics. *BJU Int*. 2013;112(5):568-577.
- Kroenig M, Schaal K, Benndorf M, et al. Diagnostic accuracy of robot-guided, software based transperineal MRI/TRUS fusion biopsy of the prostate in a high risk population of previously biopsy negative men. *BioMed Res Int*. 2016;2016:1-6.
- Yu X, Lou B, Shi B, et al. False positive reduction using multiscale contextual features for prostate cancer detection in multiparametric MRI scans. Paper presented at: IEEE 17th International Symposium on Biomedical Imaging (ISBI); 3-7 April 2020. 2020.
- Epstein JI, Egevad L, Amin MB, Delahunt B, Srigley JR, Humphrey PA. The 2014 International Society of Urological Pathology (ISUP) Consensus Conference on Gleason grading of

- prostatic carcinoma: definition of grading patterns and proposal for a new grading system. *Am J Surg Pathol*. 2016;40(2):244-252.
27. Thomsen FB, Brasso K, Klotz LH, Røder MA, Berg KD, Iversen P. Active surveillance for clinically localized prostate cancer—a systematic review. *J Surg Oncol*. 2014;109(8):830-835.
 28. Klotz L. Active surveillance for prostate cancer: for whom? *J Clin Oncol*. 2005;23(32):8165-8169.
 29. Bastian PJ, Carter BH, Bjartell A, et al. Insignificant prostate cancer and active surveillance: from definition to clinical implications. *Eur Urol*. 2009;55(6):1321-1332.
 30. Fehr D, Veeraraghavan H, Wibmer A, et al. Automatic classification of prostate cancer Gleason scores from multiparametric magnetic resonance images. *Proc Natl Acad Sci*. 2015;112(46):E6265-E6273.
 31. Antonelli M, Johnston EW, Dikaios N, et al. Machine learning classifiers can predict Gleason pattern 4 prostate cancer with greater accuracy than experienced radiologists. *Eur Radiol*. 2019;29(9):4754-4764.
 32. Arif M, Schoots IG, Castillo Tovar J, et al. Clinically significant prostate cancer detection and segmentation in low-risk patients using a convolutional neural network on multi-parametric MRI. *Eur Radiol*. 2020;30(12):6582-6592.
 33. Klotz L, Zhang L, Lam A, Nam R, Mamedov A, Loblaw A. Clinical results of long-term follow-up of a large, active surveillance cohort with localized prostate cancer. *J Clin Oncol*. 2010;28(1):126-131.
 34. Ali K, Gunnar A, Jan-Erik D, Hans L, Pär L, Jonas H. PSA doubling time predicts the outcome after active surveillance in screening-detected prostate cancer: results from the European randomized study of screening for prostate cancer, Sweden section. *Int J Cancer*. 2007;120(1):170-174.
 35. Sugimoto M, Shiraishi T, Tsunemori H, et al. Pathological findings at radical prostatectomy in Japanese prospective active surveillance cohort. *Jpn J Clin Oncol*. 2010;40(10):973-979.
 36. Hettiarachchi D, Geraghty R, Rice P, et al. Can the use of serial multiparametric magnetic resonance imaging during active surveillance of prostate cancer avoid the need for prostate biopsies?—a systematic diagnostic test accuracy review. *Eur Urol Oncol*. 2021;4(3):426-436.
 37. Rajwa P, Pradere B, Quhal F, et al. Reliability of serial prostate magnetic resonance imaging to detect prostate cancer progression during active surveillance: a systematic review and meta-analysis. *Eur Urol*. 2021;80(5):549-563.
 38. Al Otaibi M, Ross P, Fahmy N, et al. Role of repeated biopsy of the prostate in predicting disease progression in patients with prostate cancer on active surveillance. *Cancer*. 2008;113(2):286-292.
 39. Schröder FH, Hugosson J, Roobol MJ, et al. Screening and prostate-cancer mortality in a randomized European study. *N Engl J Med*. 2009;360(13):1320-1328.
 40. Sushentsev N, Moreira Da Silva N, Yeung M, et al. Comparative performance of fully-automated and semi-automated artificial intelligence methods for the detection of clinically significant prostate cancer on MRI: a systematic review. *Insights Imaging*. 2022;13(1):59.
 41. Bulten W, Kartasalo K, Chen P-HC, et al. Artificial intelligence for diagnosis and Gleason grading of prostate cancer: the PANDA challenge. *Nature Med*. 2022;28(1):154-163.
 42. Barry MJ. Prostate-specific-antigen testing for early diagnosis of prostate cancer. *N Engl J Med*. 2001;344(18):1373-1377.
 43. IARC. Data visualization tools for exploring the global cancer burden in 2020.
 44. Mahal BA, Butler S, Franco I, et al. Use of active surveillance or watchful waiting for low-risk prostate cancer and management trends across risk groups in the United States, 2010-2015. *JAMA*. 2019;321(7):704-706.
 45. Eastham JA, Auffenberg GB, Barocas DA, et al. Clinically localized prostate cancer: AUA/ASTRO guideline, part I: introduction, risk assessment, staging, and risk-based management. *J Urol*. 2022;208(1):10-18.
 46. Willemse PPM, Davis NF, Grivas N, et al. Systematic review of active surveillance for clinically localised prostate cancer to develop recommendations regarding inclusion of intermediate-risk disease, biopsy characteristics at inclusion and monitoring, and surveillance repeat biopsy strategy. *Eur Urol*. 2022;81(4):337-346.
 47. Litjens G, Debats O, Barentsz J, Karssemeijer N, Huisman H. Computer-aided detection of prostate cancer in MRI. *IEEE Trans Med Imaging*. 2014;33(5):1083-1092.
 48. Sunoqrot MRS, Saha A, Hosseinzadeh M, Elschot M, Huisman H. Artificial intelligence for prostate MRI: open datasets, available applications, and grand challenges. *Eur Radiol Experimental*. 2022;6(1):35.

How to cite this article: Oerther B, Engel H, Nedelcu A, et al. Prediction of upgrade to clinically significant prostate cancer in patients under active surveillance: performance of a fully automated AI-algorithm for lesion detection and classification. *The Prostate*. 2023;83:871-878. doi:10.1002/pros.24528